

# Coexpression of Tim-3 and PD-1 identifies a CD8<sup>+</sup> T-cell exhaustion phenotype in mice with disseminated acute myelogenous leukemia

Qing Zhou,<sup>1</sup> Meghan E. Munger,<sup>1</sup> Rachele G. Veenstra,<sup>1</sup> Brenda J. Weigel,<sup>1</sup> Mitsuomi Hirashima,<sup>2</sup> David H. Munn,<sup>3</sup> William J. Murphy,<sup>4</sup> Miyuki Azuma,<sup>5</sup> Ana C. Anderson,<sup>6</sup> Vijay K. Kuchroo,<sup>6</sup> and Bruce R. Blazar<sup>1</sup>

<sup>1</sup>Masonic Cancer Center and Department of Pediatrics, Division of Hematology/Oncology and Blood and Marrow Transplantation and <sup>2</sup>Department of Immunology and Immunopathology, Faculty of Medicine, Kagawa University, Kagawa, Japan; <sup>3</sup>Department of Pediatrics, School of Medicine, Medical College of Georgia, Augusta, GA; <sup>4</sup>Department of Dermatology, University of California, Davis, CA; <sup>5</sup>Department of Molecular Immunology, Tokyo Medical and Dental University, Tokyo, Japan; and <sup>6</sup>Center for Neurologic Diseases, Brigham and Women's Hospital, Harvard Medical School, Boston, MA

**Tumor-associated immune suppression can lead to defective T cell-mediated anti-tumor immunity. Here, we identified a unique phenotype of exhausted T cells in mice with advanced acute myelogenous leukemia (AML). This phenotype is characterized by the coexpression of Tim-3 and PD-1 on CD8<sup>+</sup> T cells in the liver, the major first site of AML metastases. PD-1 and Tim-3 coexpression increased during AML progression. PD-1<sup>+</sup>Tim-3<sup>+</sup> CD8<sup>+</sup> T cells were deficient in their ability to**

**produce IFN- $\gamma$ , TNF- $\alpha$ , and IL-2 in response to PD-1 ligand (PDL1) and Tim-3 ligand (galectin-9) expressing AML cells. PD-1 knockout (KO), which were partially resistant to AML challenge, up-regulated Tim-3 during AML progression and such Tim-3<sup>+</sup>PD-1- KO CD8<sup>+</sup> T cells had reduced cytokine production. Galectin-9 KO mice were more resistant to AML, which was associated with reduced T-regulatory cell accumulation and a modest induction of PD-1 and Tim-3 expression on**

**CD8<sup>+</sup> T cells. Whereas blocking the PD-1/PDL1 or Tim-3/galectin-9 pathway alone was insufficient to rescue mice from AML lethality, an additive effect was seen in reducing—albeit not eliminating—both tumor burden and lethality when both pathways were blocked. Therefore, combined PD-1/PDL1 and Tim-3/galectin-9 blockade may be beneficial in preventing CD8<sup>+</sup> T-cell exhaustion in patients with hematologic malignancies such as advanced AML. (*Blood*. 2011;117(17):4501-4510)**

## Introduction

T-cell exhaustion, a state of T-cell dysfunction characterized by diminished cytokine production, impaired killing, and hypoproliferation, was first characterized in the settings of chronic lymphocytic choriomeningitis virus (LCMV) infection.<sup>1,2-5</sup> Since its discovery, the process of T-cell exhaustion has been of intense interest and has been the subject of study in viral infections such as hepatitis C virus<sup>2,6</sup> and HIV,<sup>3,7</sup> as well as in tumor models.<sup>8,9,10,11</sup> Cell-surface antigen determinants such as program death-1 (PD-1), CTLA-4, and, in some instances, CD28 (eg, hepatitis C viral infection) can be used to identify antigen-specific T cells that are at an exhaustion stage.<sup>4</sup>

T-cell immunoglobulin and mucin domain-containing protein 3 (Tim-3) is a type I membrane glycoprotein and its expression can be found on terminally differentiated Th1 cells and innate immune cells.<sup>12-14</sup> Galectin-9 (gal-9) is its only confirmed Tim-3 ligand to date,<sup>15,16</sup> although it is known that Tim-3 can also bind to certain carbohydrate moieties.<sup>17</sup> Ligation of Tim-3 on T cells and gal-9 inhibits Th1 responses and plays an important role in infection, autoimmunity, peripheral tolerance, and inflammation.<sup>14,18-21</sup> In addition to its negative regulatory role in dampening the immune system, a recent report showed a synergistic effect of Tim-3 signaling and lipopolysaccharide in producing proinflammatory cytokines by naive dendritic cells (DCs) and monocytes,<sup>22</sup> indicating a dual role of the Tim-3 signaling pathway at a different phase of immune responses.

Studies have demonstrated a strong correlation between PD-1 and Tim-3 coexpression and a more severe exhaustion phenotype of CD8<sup>+</sup>

T cells during chronic LCMV infection<sup>23</sup> and, most recently, Friend leukemia infection,<sup>24</sup> leading to a search for an exhaustion phenotype in other settings of chronic antigenic stimulation. Very recently, a PD-1<sup>+</sup>/Tim-3<sup>+</sup> CD8<sup>+</sup> T-cell exhaustion phenotype was identified in murine solid tumor model systems.<sup>25</sup> Within the local milieu of the solid tumor, proteins produced by the tumor cells often render the microenvironment highly suppressive by altering immune cells contained within the microenvironment and by recruitment of immune-suppressor cells to that microenvironment. As such, it is not surprising that solid tumor models favor a state of exhaustion for tumor-infiltrating lymphocytes. Despite the progress made on understanding the biologic consequences of the expression of PD-1 or Tim-3 on T-cell function, the link between Tim-3 and PD-1 in nonsolid tumor such as acute myelogenous leukemia (AML) has not yet been defined. The systemic nature of AML and the capacity of AML cells to serve as APCs should decrease the likelihood of a profound state of T-cell exhaustion that has been seen with solid tumor models. Given the role of the PD-1/Tim-3 phenotype in the immune response in a Friend leukemia virus infection<sup>24</sup> and in distinct solid tumor models and the important potential differences among chronic viral infection, solid tumors, and hematologic malignancies, it is crucial to determine whether AML cells can express relevant ligands for exhausted T cells and if so, to further determine whether T cells exposed to such AML cells develop an exhaustion phenotype. Only with such data can a foundation be set for interventional studies in patients with disseminated AML.

Submitted September 30, 2010; accepted February 17, 2011. Prepublished online as *Blood* First Edition paper, March 8, 2011; DOI 10.1182/blood-2010-10-310425.

The online version of this article contains a data supplement.

The publication costs of this article were defrayed in part by page charge payment. Therefore, and solely to indicate this fact, this article is hereby marked "advertisement" in accordance with 18 USC section 1734.

© 2011 by The American Society of Hematology

Previous studies by us<sup>26</sup> and others<sup>11</sup> have indicated that the PD-1/PDL1 pathway clearly is important in murine AML resistance. However, because PD-1 knockout (KO) mice were only partially resistant to AML cells, we hypothesized that other pathway(s) may be involved in preventing a more robust response against this tumor type. Therefore, in the present study, we examined the collaborative role of PD-1 and Tim-3 in tumor-associated T-cell exhaustion in a murine model of advanced AML in which the AML cells expressed both PDL1 and the Tim-3 ligand, gal-9. In wild-type (WT) mice, PD-1 and Tim-3 was found to be coexpressed on CD8<sup>+</sup> T cells in the liver, the major first site of metastases and a known site of immune suppression in AML,<sup>11,12,26</sup> and this coexpression increased during AML progression. PD-1<sup>+</sup>Tim-3<sup>+</sup> CD8<sup>+</sup> T cells were deficient in their ability to produce cytokines (IFN- $\gamma$ , TNF- $\alpha$ , IL-2). Gal-9 KO mice challenged with the gal-9<sup>+</sup> AML cells were more resistant than WT mice to AML, which was associated with reduced T-regulatory cell (Treg) accumulation and induction of PD-1 and Tim-3 expression on CD8<sup>+</sup> T cells. Whereas blocking the interaction of either PD-1/PDL1 or Tim-3/gal-9 alone was insufficient to rescue mice from AML, an additive effect was seen in reducing AML tumor burden and prolonging survival when both pathways were blocked. Combined PD-1/PDL1 and Tim-3/gal-9 blockade represents a novel approach and the current studies provide the first definitive foundation of such therapy to rescue CD8<sup>+</sup> T-cell exhaustion in patients with hematologic malignancies such as advanced AML.

## Methods

### Mice

C57BL/6 (termed B6, H2<sup>b</sup>) mice, 7-12 weeks old at study, were obtained from the National Institutes of Health (NIH; Bethesda, MD). B6 gal-9 KO mice<sup>27,28</sup> were kindly provided by GalPharma Co Ltd. B6 PD-1 KO mice<sup>29</sup> were provided by Drs Tasuku Honjo and Hiroyuki Nishimura (Kyoto University, Kyoto, Japan). Gal-9 KO and PD-1 KO were maintained in the animal facility at the University of Minnesota. Mice were housed in micro-isolator cages under specific pathogen-free conditions. All experiments were conducted under approved institutional animal care and use committee protocols at the University of Minnesota (Minneapolis, MN).

### Abs and in vivo AML model

C1498FFDsR, stable transfectants of C1498 (an AML cell line obtained from ATCC) that express the fluorescent *Discosoma* coral-derived protein DsRed2 and firefly luciferase, were prepared.<sup>30</sup> C1498FFDsR (10<sup>6</sup>) was injected into B6, gal-9 KO, or PD-1 KO mice through the tail vein. In some studies, 7 days after AML injection, anti-PDL1 mAb (clone MIH7, 200  $\mu$ g/dose), mTim-3 hFc (100  $\mu$ g/dose; kindly provided by Dr Terry Strom, Boston, MA),<sup>20,21</sup> or control rat IgG was injected intraperitoneally every other day from days 7 to 21. Mice were monitored for survival or killed 25 days after tumor injection for immune parameter determination by flow cytometry.

### Flow cytometry

Liver leukocytes were prepared by Percoll ingredient separation as previously described.<sup>31</sup> For cytokine detection, cells were stimulated in vitro with purified anti-CD3 (1  $\mu$ g/mL), anti-CD28 (1  $\mu$ g/mL), and Monensin solution (eBioscience) for 5 hours. Cells were then surface labeled with PD-1-FITC, Tim-3-allophycocyanin, CD8-allophycocyanin-eFluor 780, fixed and permeabilized with the Fix and Perm permeabilization kit (Invitrogen), and labeled with anti-IFN- $\gamma$ -PerCP-Cy5.5, IL-2-PE-cy7 and anti-TNF- $\alpha$ -eFluor 450. For gal-9 and Treg determination, cells were surface labeled with Gr-1-FITC, CD11b-PerCp, CD11c-allophycocyanin, CD4-V500, fixed and permeabilized with Foxp3 Fix/Perm buffers and

labeled with Foxp3-PE-cy7 and gal-9-Pacific Blue. Cells were washed in PBS containing 2% FBS and analyzed using the FACS LSRII FORTRESSA (BD Biosciences) and were gated on 20 000 live events.

### In vitro Treg suppression assay

CD4<sup>+</sup> 25br Tregs were isolated at > 90% purity from spleens of naive B6 WT or gal-9 KO mice by MACs column selection (Miltenyi Biotec). CD8<sup>+</sup> T cells from WT mice were isolated at > 90% purity by MACs column selection, and labeled with 1  $\mu$ M CFSE. T cell- and NK cell-depleted splenocytes from WT mice were used as APCs. CFSE-labeled CD8<sup>+</sup> T responder cells (5  $\times$  10<sup>4</sup>; WT or gal-9 KO) were stimulated with 1.5  $\times$  10<sup>5</sup> APCs in RPMI-c and 0.5  $\mu$ g/mL purified anti-CD3 $\epsilon$  mAb (eBioscience). Tregs (1  $\times$  10<sup>5</sup>) from WT or gal-9 KO mice were added to the culture and RPMI-c was added to the controls. Four days after coculture at 37°C, 5% CO<sub>2</sub>, cells from each condition were harvested and the proliferation was determined by CFSE dilution.

### Bioluminescent imaging studies

A Xenogen IVIS imaging system was used for live animal imaging. Firefly luciferin substrate (0.1 mL; 30 mg/mL) was injected intraperitoneally and the IVIS imaging was performed immediately after substrate injection. Data were analyzed and presented as photon counts per area.

### Statistics

The Kaplan-Meier product-limit method was used to calculate survival. Differences between groups were determined using log-rank statistics. One-way ANOVA with post-hoc Tukey test and Student *t* test unpaired comparison were used to determine significant differences between each group in bar graph. *P* values < .05 were considered to be significant.

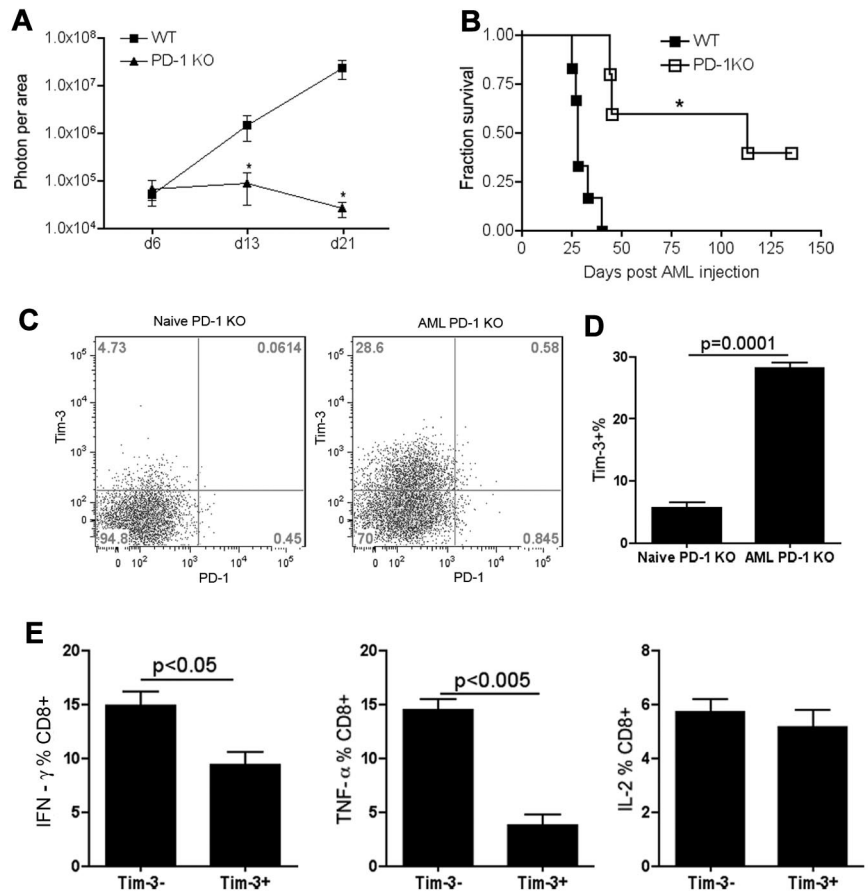
## Results

### Tim-3 is highly expressed on CD8<sup>+</sup> T cells in PD-1 KO mice

Exhausted T cells were first defined in chronic viral infections,<sup>32,33</sup> whereby they were identified by the overexpression of inhibitory receptor PD-1.<sup>8,32-34</sup> We and others have shown that high PD-1 expression on T cells in an advanced AML model is associated with low IFN- $\gamma$  production, indicative of T-cell dysfunction and immune suppression.<sup>11,26</sup> As shown here and consistent with the published literature,<sup>11,26</sup> compared with WT mice given PDL1-expressing AML cells, PD-1 KO mice had a reduced AML tumor burden (Figure 1A), leading to significantly prolonged survival (Figure 1B). However, even though PD-1 up-regulation is associated with T-cell dysfunction in mice with advanced AML, the majority of PD-1 KO mice still succumbed to AML (Figure 1B). Therefore, we hypothesized that the expression of other pathways may be contributing to the failure of complete AML resistance and the possible acquisition of a T-cell exhaustion phenotype even in the absence of PD-1 expression.

Recent studies have indicated an important regulatory role of Tim-3/gal-9 pathway in the immune response.<sup>12,15,20,21,35</sup> Thus, we explored the possibility that the Tim-3/gal-9 pathway may be involved in the T-cell dysfunction in advanced AML. To determine whether Tim-3 signaling is involved in AML-induced immunosuppression, Tim-3 expression was assessed in PD-1 KO mice 25 days post-AML injection and compared with naive PD-1 KO mice. In AML-bearing PD-1 KO mice, Tim-3 was found to be highly expressed on CD8<sup>+</sup> T cells in the liver, the major target organ of initial C1498FFDsR dissemination (Figure 1C-D). Compared with the Tim-3<sup>-</sup> fraction, the Tim-3<sup>+</sup> fraction of PD-1 KO CD8<sup>+</sup> T cells had a significant reduction in their capacity to produce proinflammatory

**Figure 1. AML-induced Tim-3-expressing liver CD8<sup>+</sup> T cells in PD-1 KO mice were dysfunctional.** (A-B) WT or PD-1 KO mice (10 mice/group) were injected with 10<sup>6</sup> C1498FFDsR through the tail vein. (A) Whole-body imaging was performed 7, 14, and 21 days post-AML injection. PD-1 KO mice had decelerated tumor growth compared with WT controls. \**P* < .01 compared with WT controls. (B) Significant prolonged surviving time with partial survival from AML was attained in PD-1 KO mice. \**P* < .001 compared with WT controls. (C-E) Naive or AML-bearing PD-1 KO mice (3-4 mice/group) were killed 25 days post-AML injection. Liver leukocytes were isolated. Tim-3 and intracellular cytokine production was determined by FACS. Tim-3 expression induced by AML on the liver CD8<sup>+</sup> T cells in PD-1 KO mice 25 days post-AML injection is shown in flow dot plot (C) and bar graph (D). (E) Tim-3<sup>+</sup>CD8<sup>+</sup> T cells from PD-1 KO mice were deficient in producing IFN- $\gamma$ , TNF- $\alpha$  but not IL-2 compared with Tim-3<sup>-</sup> fraction.



cytokines such as IFN- $\gamma$  and TNF- $\alpha$  without differences in IL-2 secretion (Figure 1E), hallmarks of a T-cell exhaustion phenotype.

#### Tim-3- and PD-1-coexpressing CD8 T cells in WT AML-bearing mice are dysfunctional

The above data suggested that both the Tim-3/gal-9 and PD-1/PDL1 pathways might be involved in AML-associated immune suppression. Therefore, we quantified the coexpression of Tim-3 and PD-1 on CD8<sup>+</sup> T cells in WT mice. Approximately 20% CD8<sup>+</sup> T cells in the liver coexpressed PD-1 and Tim-3, whereas there was only minimal expression of either Tim-3 (1%-3%) or PD-1 (2%-4%) alone (Figure 2A-B). Coexpression of PD-1 and Tim-3 was also observed on the CD8<sup>+</sup> T cells in the BM and the spleen, 2 other AML metastasis sites with less tumor dissemination (supplemental Figure 1, available on the Blood Web site; see the Supplemental Materials link at the top of the online article). The level of PD-1 and Tim-3 coexpression was less in the spleen (3%-7%) and variable in the BM (20%-40%). In contrast to CD8<sup>+</sup> T cells, the expression of either PD-1 or Tim-3 was not observed on CD4<sup>+</sup> T cells in mice challenged with these MHC class I<sup>+</sup>II<sup>-</sup> AML cells (data not shown). In AML tumor-bearing mice, the expression of Tim-3 had a comparable time course as PD-1<sup>26</sup> with a peak of Tim-3 expression at the late phase of disease (> day 20, Fig. 2C). The expression of Tim-3 on CD8<sup>+</sup> T cells was significantly higher in PD-1 KO mice compared with WT mice at 25 days after AML injection (Figure 2D-E). In AML-bearing mice, whereas PD-1<sup>-</sup>Tim-3<sup>-</sup> CD8<sup>+</sup> T cells were predominantly (68%) naive (CD62L<sup>+</sup>CD44<sup>-lo</sup>), Tim-3<sup>+</sup>PD-1<sup>+</sup> CD8<sup>+</sup> T cells were predominantly (66%) effector cells (CD62L<sup>-</sup>CD44<sup>hi</sup>; Figure 2F). These data suggested that the exhaustion phenotype occurred in CD8<sup>+</sup> T cells, located at the site

of disease and generated as the consequence of an ongoing, vigorous response to the AML cells, some of which are likely tumor-reactive whereas others may be a reflection of global immune suppression. No differences were seen in the frequency of central memory (CD62L<sup>+</sup>, CD44<sup>+</sup>) CD8<sup>+</sup> T cells. CD8<sup>+</sup> T cells coexpressing Tim-3 and PD-1 had a significantly decreased percentage of IFN- $\gamma$ , TNF- $\alpha$  as well as IL-2-producing compared with T cells that did not express either Tim-3 or PD-1 (Figure 2G). Collectively, these data suggested that advanced AML leads to a marked increase in CD8<sup>+</sup> T cells with a CD8<sup>+</sup> T-effector cell phenotype denoted by exhaustion characteristics.

#### Gal-9 is highly expressed by AML and host immune cells

Tim-3/gal-9 interactions play a critical role in regulating immune cell homeostasis and inflammatory response.<sup>18,36</sup> In addition to Tim-3, gal-9 has also been shown to bind to CD44 directly and inhibit CD44-hyaluronan-mediated T-cell migration in an asthma model.<sup>37</sup> Gal-9 has been shown to be expressed on immune cells,<sup>38,39</sup> parenchymal cells<sup>40</sup> and some types of human and mouse tumor cells.<sup>25,38,41,42</sup> Whereas some studies have suggested that gal-9 expression by tumor cells results in reduced metastatic potential,<sup>43</sup> other recent studies have indicated that gal-9 expression on tumor cells may increase tumorigenicity by promoting T-cell dysfunction.<sup>25,41</sup>

To determine whether gal-9 expression by AML cells may be contributing to the exhaustion function of Tim-3<sup>+</sup>PD-1<sup>+</sup> CD8<sup>+</sup> T cells, we assayed the AML cell line used here C1498FFDsR cells, for gal-9 expression. Flow cytometric analysis indicated that gal-9 was expressed at high levels on AML C1498FFDsR cells (Figure 3A). Although IFN- $\gamma$  is known to up-regulate gal-9

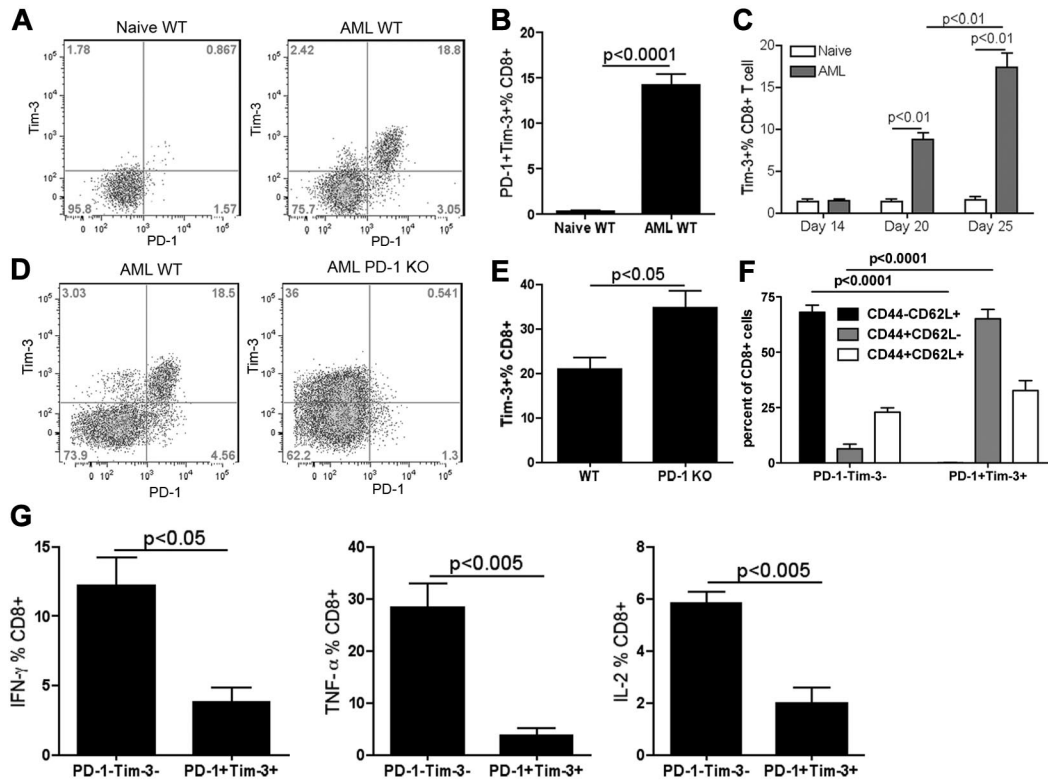


**Figure 2. AML-induced PD-1<sup>+</sup>Tim-3<sup>+</sup> liver CD8<sup>+</sup> T cells in WT mice were dysfunctional.** (A-C) B6 WT mice were injected intravenously with  $10^6$  C1498FFDsR. Liver leukocytes were isolated 14, 20, and 25 days post-AML injection. PD-1 and Tim-3 expression was determined by FACS. PD-1 and Tim-3 coexpression detected on liver CD8<sup>+</sup> T cells 25 days post-AML injection is shown in flow dot plot (A) and bar graph (B). (C) Time course of Tim-3 expression on liver CD8<sup>+</sup> T cells as AML progression in mice is shown. Tim-3 was up-regulated at a late phase of disease (day 20 and 25 but not day 14). (D-F) WT and PD-1 KO mice (3-4 mice/group) were injected with  $10^6$  C1498FFDsR. Liver leukocytes were isolated 25 days post-AML injection. PD-1, Tim-3, CD44, CD62L, and intracellular cytokine production was determined by flow cytometry. (D-E) Tim-3 was expressed at a higher level in PD-1 KO mice compared with WT mice. (F) Majority of PD-1<sup>+</sup>Tim-3<sup>+</sup> CD8<sup>+</sup> T cells were CD44<sup>-</sup>CD62L<sup>-</sup>, while PD-1<sup>-</sup>Tim-3<sup>-</sup> CD8<sup>+</sup> T cells were mainly CD44<sup>-</sup>CD62L<sup>+</sup>. (G) PD-1<sup>-</sup> and Tim-3-coexpressing CD8<sup>+</sup> T cells from WT mice are highly deficient in producing IFN- $\gamma$ , TNF- $\alpha$  and IL-2 compared with PD-1-Tim-3- fraction. Data were pooled from 2 individual experiments.

expression<sup>39,44,45</sup> (eg, mouse CD11b<sup>+</sup> cells, HUVECs, and human dermal fibroblasts), IFN- $\gamma$  treatment (1000 ng/mL) in vitro for 48 hours did not further up-regulate gal-9 expression (Figure 3A).

Similar to PDL1, expression of gal-9 is widely distributed in a multitude of organs in non-tumor-bearing mice.<sup>40</sup> Therefore, different immune cell types in non-tumor-bearing and AML-bearing mice were analyzed for gal-9 expression. In non-tumor-bearing mice, the percentage and MFI of gal-9 expression was the highest in the liver, followed by the spleen and BM (Figure 3B). The percentage and MFI of gal-9 expression remained same in AML-bearing mice (Figure 3B). However, in mice with advanced AML, the number of gal-9-expressing CD11c<sup>+</sup> DCs, CD11b<sup>+</sup>Gr-1<sup>-</sup> myeloid cells and CD11b<sup>+</sup>Gr-1<sup>+</sup> myeloid-derived suppressor cells increased in the liver (Figure 3C). In addition, the absolute number of both CD11c<sup>+</sup> and CD11b<sup>+</sup>Gr-1<sup>+</sup> cells increased in the spleen and the number of CD11c<sup>+</sup> increased in the BM (Figure 3C). Therefore, the tumors themselves as well as host immunostimulatory and immune-inhibitory cells are a source of gal-9 for the signaling of Tim-3<sup>+</sup> CD8<sup>+</sup> T cells.

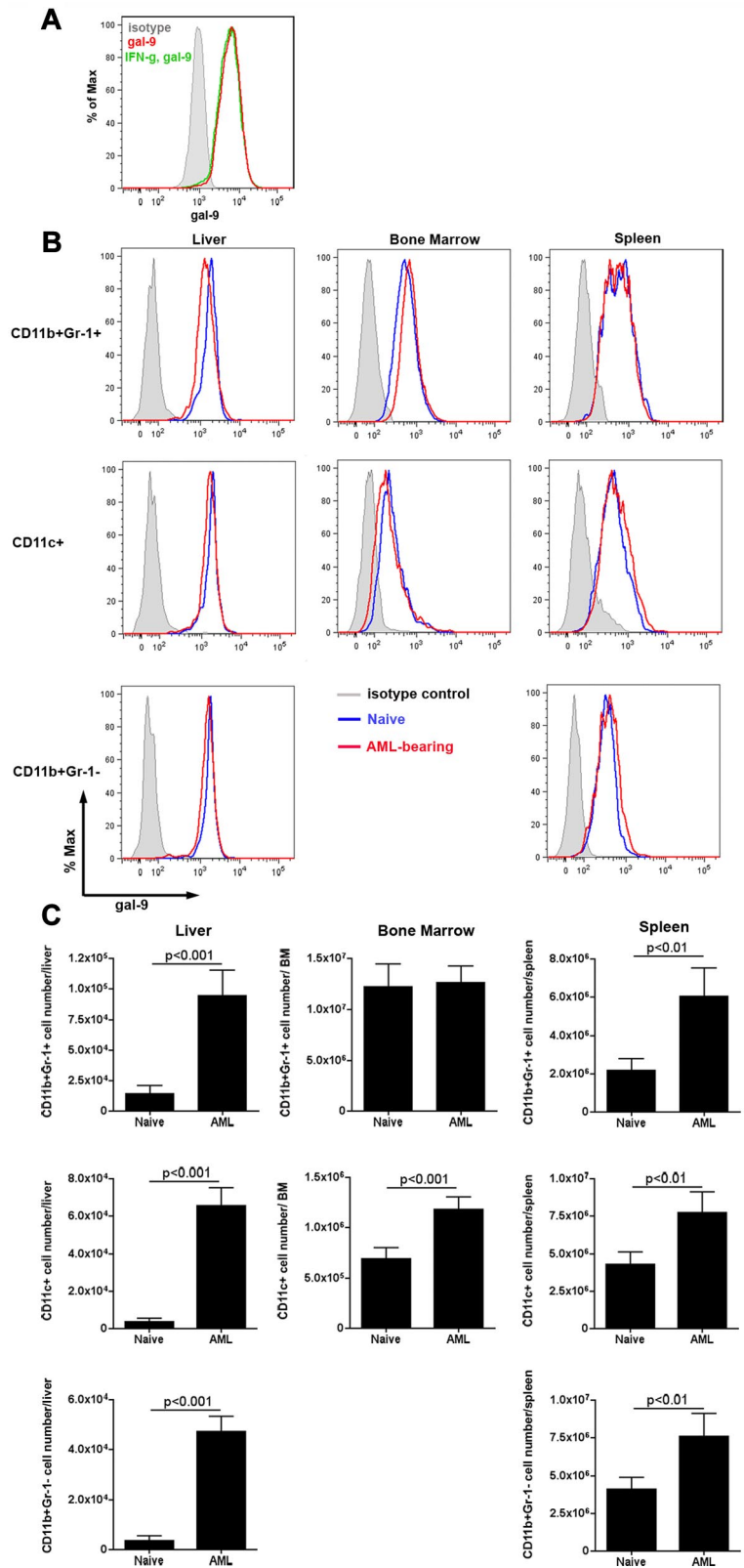
#### Gal-9 KO mice are more resistant to AML

Studies to date have not addressed the issue as to whether the expression of gal-9 by the tumor cells themselves can contribute to the exhaustion phenotype. Therefore, gal-9 KO and WT mice were given gal-9<sup>+</sup> AML cells and tumor burden and survival monitored. As tumor progressed, gal-9 KO mice had a lower tumor burden as assessed on days 14 and 21, but not day 28, after tumor injection.

The lower tumor burden, as assessed by bioluminescent imaging (BLI), at these earlier time points resulted in significantly (*P* < .01, Figure 4B) prolonged survival in gal-9 KO versus WT mice, although mice were not cured from AML. Thus, gal-9 KO mice were relatively but not absolutely resistant to AML.

In mice with advanced AML, host Tregs accumulate and inhibit antitumor effector cell function.<sup>31</sup> Previously, we have shown that PD-1 KO recipients, also relatively resistant to AML, had defective Treg function, which may have accounted in part for decreased AML tumorigenicity. Gal-9 has been shown to be expressed on activated Tregs,<sup>46</sup> although the effect of gal-9 expression on Treg generation and function in murine tumor models has not been reported to date. To determine whether gal-9 KO mice have normal Tregs, the percentage and function of Tregs were determined in naive and AML-bearing gal-9 KO versus WT mice. In contrast to PD-1 KO mice,<sup>26</sup> naive gal-9 KO and WT mice have a comparable fraction of Tregs. As we have reported,<sup>31</sup> AML-bearing WT mice have a higher percentage of Tregs versus non-tumor-bearing WT mice. In marked contrast, the percentage of Tregs in the liver of AML-bearing gal-9 KO mice remained similar to naive gal-9 KO mice 25 days after AML injection. To determine whether gal-9 KO Tregs are functional, an in vitro suppression assay was performed. In contrast to Tregs isolated from PD-1 KO mice, which are defective in their in vitro suppressive capacity, gal-9 KO Tregs could inhibit CD8<sup>+</sup> T-cell proliferation to a similar extent as WT Tregs (Figure 4D), suggesting Treg function was intact in gal-9 KO mice.

**Figure 3. Gal-9 is expressed on C1498FFDsR cells and immune cells.** C1498FFDsR cells were untreated or treated with IFN- $\gamma$  (1000 ng/mL) for 48 hours. Gal-9 expression was assessed by flow cytometry as described. (A) C1498FFDsR cells express gal-9 (> 90%). IFN- $\gamma$  treatment (1000 U/mL, 48 hours) did not alter the expression of gal-9 on C1498FFDsR cells. B6 mice were injected intravenously with 10<sup>6</sup> C1498FFDsR. (B-C) Leukocytes from the liver, BM, and spleen of either naive or AML-bearing B6 mice (4 mice/group, 25 days post-AML injection) were prepared. Gal-9 expression was determined by flow cytometry. (B) Flow histogram graph of gal-9 expression on CD11b<sup>+</sup>Gr-1<sup>+</sup>, CD11c<sup>+</sup>, and CD11b<sup>+</sup>Gr-1<sup>-</sup> cells from the liver, BM, and spleen are shown. Gal-9 is expressed on all 3 types of cells in various organs measured (blue). The presence of AML (red) did not change the pattern of gal-9 expression (blue) in all 3 organs. (C) Bar graphs of the total number of gal-9 expressing CD11b<sup>+</sup>Gr-1<sup>+</sup>, CD11c<sup>+</sup>, and CD11b<sup>+</sup>Gr-1<sup>-</sup> cells in the liver, BM, and spleen from naive or AML-bearing mice are shown.



Because a Treg defect was unlikely to explain the relative resistance of gal-9 KO mice to AML challenge, we next sought to determine whether gal-9 KO mice given AML cells had a comparable proportion of Tim-3<sup>+</sup>PD-1<sup>+</sup> exhausted CD8<sup>+</sup> T cells. In gal-9 KO mice, the percentage of PD-1<sup>+</sup>Tim-3<sup>+</sup> CD8<sup>+</sup> T cells in the liver of AML-bearing versus non-tumor-bearing mice was

increased (AML gal-9 KO vs naive gal-9 KO,  $P < .05$ , Figure 4E). However, the up-regulation of PD-1 and Tim-3 in gal-9 KO mice was modest compared with AML-bearing WT mice (AML WT vs AML gal-9 KO,  $P < .01$ , Figure 4E). Similar to WT mice, PD-1<sup>+</sup>Tim-3<sup>+</sup> CD8<sup>+</sup> T cells in AML-bearing gal-9 KO mice were deficient in IFN- $\gamma$ , TNF- $\alpha$ , and IL-2 production (Figure 4F).

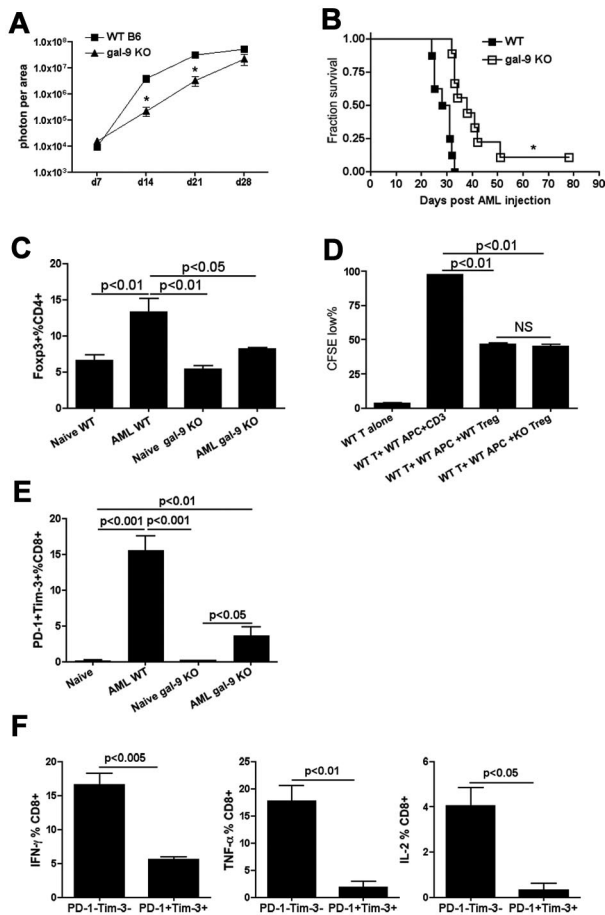


**Figure 4. Gal-9 KO mice were more resistant to AML.** (A-B) B6 WT or gal-9 KO mice (10 mice/group) were injected intravenously with  $10^6$  C1498FFDsR. (A) Whole-body imaging was performed on 7, 14, 21, and 28 days post-AML injection (10 mice/group). Gal-9 KO mice had a slower tumor growth compared with WT mice 14 and 21 days post-AML injection. Tumor burden was equal at a later phase of disease (day 28). (B) gal-9 KO mice had a significant prolonged survival from AML. (C-E) Naive or AML-bearing gal-9 KO mice (3-4 mice/group) were killed 25 days post-AML injection. Liver leukocytes were isolated for flow cytometry. (C) The percentage of Fc $\gamma$ R3 $^+$  Tregs in CD4 $^+$  T cells from liver of AML-bearing gal-9 KO mice was similar to naive WT or gal-9 KO mice, while AML induced an increase in percentage of Fc $\gamma$ R3 $^+$  Tregs in WT mice. (D) An in vitro Treg suppression assay was performed with WT and gal-9 KO Tregs. Gal-9 KO Tregs could inhibit CD8 $^+$  T cells proliferation at a comparable level to WT Tregs. Data were pooled from 2 individual experiments (7 mice total). (E) The percentage of PD-1 $^+$ Tim-3 $^+$  CD8 $^+$  T cells was increased in the liver of AML-bearing gal-9 KO mice but to a lesser extent than in AML-bearing WT mice. Data were pooled from 2 individual experiments (7 mice total). (F) Impaired IFN- $\gamma$ , TNF- $\alpha$ , and IL-2 production was found in PD-1 $^+$ Tim-3 $^+$  CD8 $^+$  T cells in AML-bearing gal-9 KO mice. Data were pooled from 2 individual experiments (6 mice total).

Therefore, a reduced level of AML-associated Treg accumulation and PD-1/Tim-3 up-regulation may each have contributed to the enhanced antitumor immune response found in gal-9 KO mice.

#### Anti-PDL1 treatment rescued gal-9 KO mice from AML

We considered the possibility that the coexpression of PD-1 and Tim-3 on CD8 $^+$  T cells from AML-bearing mice is nonredundant in regulating the CD8 $^+$  T-cell immune response. In that event, inhibiting both signaling pathways may be necessary to restore the function of PD-1/Tim-3-coexpressing T cells in this model system. To test this hypothesis, gal-9 KO or WT mice were injected with AML cells and treated with anti-PDL1 mAb. In this system, the only source of gal-9 was from the AML cells. Live animal whole-body BLI was used to determine tumor burdens. Consistent

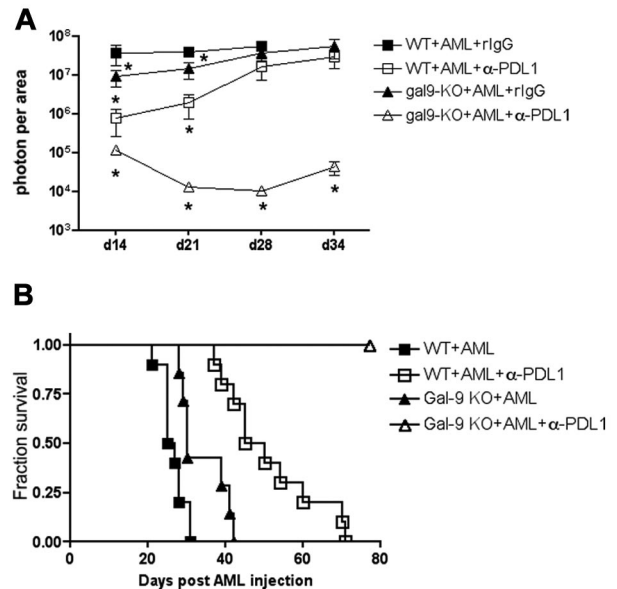


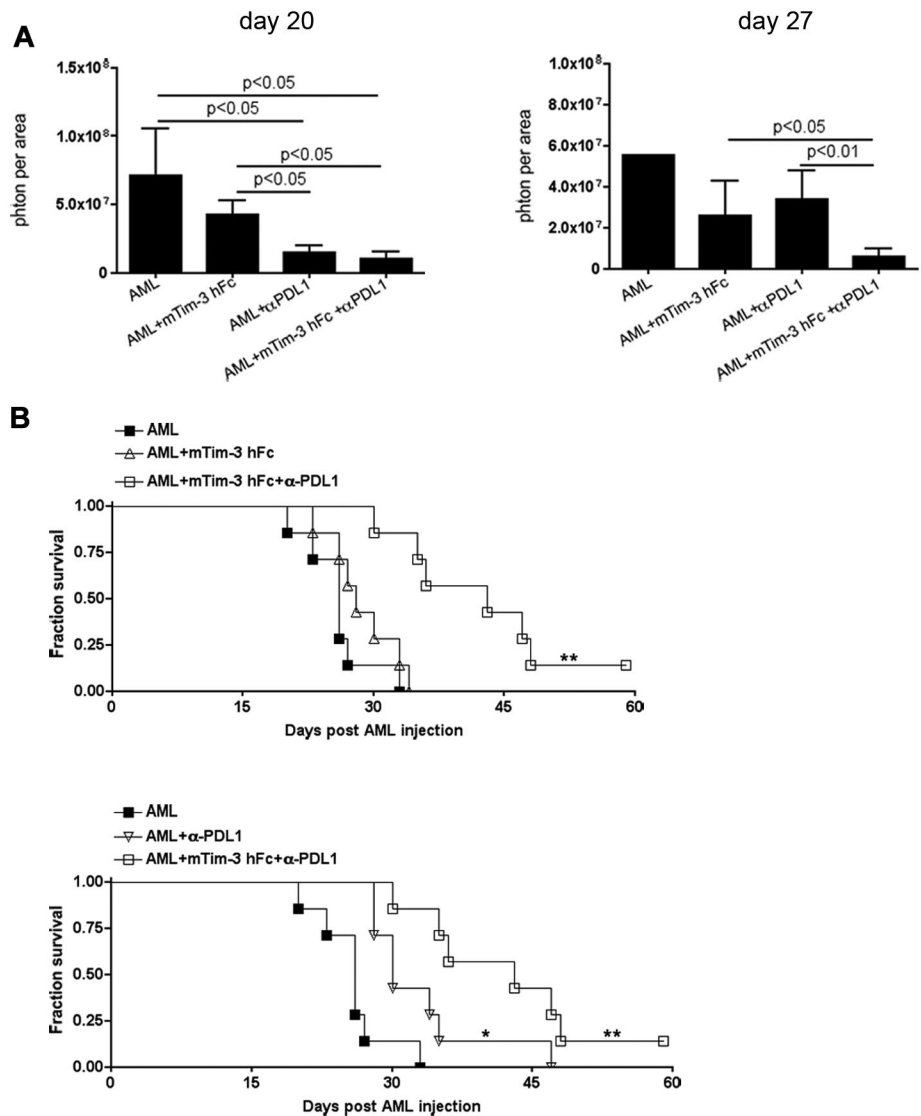
**Figure 5. Anti-PDL1 mAb treatment restored CD8 $^+$  T-cell function and rescued gal-9 KO mice from AML.** WT or gal-9 KO mice (10 mice/group) were injected iv with  $10^6$  C1498FFDsR cells. Anti-PDL1 mAb or control rIgG was administered as described. (A) Anti-PDL1 mAb treatment significantly reduced tumor burdens in WT mice 14 and 21 days post-AML injection. Gal-9 KO mice had a more dramatic decrease in tumor burdens on days 14, 21, 28, and 34, compared with WT mice. (B) Anti-PDL1 treatment prolonged the survival of AML-bearing WT mice ( $\square$  vs  $\blacksquare$ ,  $P < .0001$ ). Gal-9 KO mice had an increased survival from AML compared with WT mice ( $\blacktriangle$  vs  $\blacksquare$ ,  $P < .05$ ). Gal-9 KO mice were protected from AML by anti-PDL1 treatment and remained tumor-free by 60 days ( $\triangle$  vs  $\blacksquare$ ,  $P < .0001$ ).

with studies demonstrated in Figure 4A, gal-9 KO had a significantly ( $P < .01$ ) lower tumor burden compared with the WT mice 14 and 21 days after AML injection (Figure 5A). Anti-PDL1 versus irrelevant mAb treatment significantly ( $P < .001$ ) reduced tumor burden in WT mice at similar times after AML injection as in gal-9 KO mice (Figure 5A). The magnitude of tumor inhibition was significantly ( $P < .01$ ) greater in anti-PDL1 mAb-treated WT mice compared with irrelevant mAb-treated gal-9 KO mice (Figure 5A). More importantly, the administration of anti-PDL1 mAb in gal-9 KO mice completely eliminated the established tumor and resulted in 100% survival throughout the duration of the study (Figure 5B), the first such curative therapy we have seen under these AML tumor conditions.

#### Blockade of both Tim-3 and PD-1 pathways had an additive effect in inhibiting tumor growth

The above data indicated that the absence of gal-9 expression in the host, when coupled with anti-PDL1 mAb, resulted in the elimination of PDL1 $^+$  and gal-9 $^+$  AML cells. However, gal-9 KO mice have reduced Treg numbers and a more modest up-regulation of PD-1/Tim-3 on CD8 $^+$  T cells compared with WT mice. To develop a more clinically relevant approach, WT mice were treated with a Tim-3 fusion protein (mTim-3 hFc), anti-PDL1 blocking mAb, or the combination of both after the establishment of AML for a period of 10 days when tumor burden was high. Live animal whole-body imaging revealed that mTim-3 hFc alone failed to significantly reduce tumor burden at all 3 time points (day 14 [not shown]; day 20 and day 27: Figure 6A) and therefore failed to rescue mice from AML (Figure 6B). Mice treated with anti-PDL1 mAb had significantly less tumor burden on day 14 (not shown) and day 20 but not day 27 after AML injection; the reduction in tumor burden at the earlier time points was associated with a

**Figure 6. Combined mTim-3 hFc and anti-PDL1 treatment had an additive antitumor effect in an established AML model.** B6 mice (10 mice/group) were injected iv with  $1 \times 10^6$  C1498FFDsR cells. Ten days after AML injection, mice were treated with mTim-3 hFc (100  $\mu$ g/dose), anti-PD-L1 (200  $\mu$ g/dose) or combination of both every other day for total of 5 doses. (A) Bioluminescence imaging was performed 14 (not shown), 20 and 27 days post-AML injection (10 mice/group). Mice treated with mTim-3 hFc alone had similar tumor burden to nontreated controls. Anti-PD-L1 mAb single treatment significantly reduced tumor burden on days 14 (not shown) and 20. Mice receiving the combination therapy had decreased tumor burdens at all 3 time points. (B) mTim-3 hFc treatment did not alter the survival of AML-bearing mice. Anti-PD-L1 mAb alone significantly prolonged survival from AML compared with controls ( $\nabla$  vs  $\blacksquare$ ,  $P < .01$ ). Combined therapy had superior effect on the survival over either treatment alone ( $\square$  vs  $\triangle$  and  $\nabla$ ,  $P < .01$ ). Survival analysis was plotted according to the Kaplan-Meier method, and statistical differences were determined with the log-rank test. Error bar represents SEM.



significantly prolonged survival compared with controls ( $P < .05$ , Figure 6B). Combined anti-PDL1 mAb and mTim-3 hFc resulted in a significant reduction in tumor burden at all time points (day 14: not shown; days 20 and 27 shown in Figure 6A), and a superior survival advantage over either treatment alone ( $P < .05$ , Figure 6B). These data indicate an additive effect of Tim-3/gal-9 and PD-1/PDL1 coblockade in WT mice with advanced AML.

### Discussion

In this study, we show for the first time in a systemic hematopoietic tumor model, that Tim-3 and PD-1 coexpression demarcate a CD8<sup>+</sup> T-cell population that is exhausted. PD-1 and Tim-3 coexpression was acquired predominantly at the late phase of tumor progression. These PD-1<sup>+</sup>Tim-3<sup>+</sup> CD8<sup>+</sup> T cells were highly dysfunctional and had markedly reduced cytokine production. PD-1 KO and gal-9 KO mice each had delayed tumor growth and improved survival after challenge with AML, although the majority of mice were not cured. The exhaustion phenotype occurred in gal-9 KO mice in which the only source of gal-9 was on the AML cells themselves. We further show for the first time that gal-9 KO mice have intact

Treg function but fail to accumulate Tregs during AML progression. Most importantly, combined blockade of both the PD-1/PDL1 and Tim-3/gal-9 pathways in WT as well as gal-9 KO mice had additive effects in impeding the tumor growth and reducing but not eliminating AML-induced lethality. These results demonstrate that both PD-1 and Tim-3 pathways contribute to CD8<sup>+</sup> T-cell dysfunction in the context of advanced AML, and suggest that combined blockade may be needed to reverse the exhaustion phenotype in the clinic.

Several signaling pathways are shown to be engaged in the process of T-cell exhaustion during viral infection including PD-1/PDL1, Tim-3/gal-9, and the CD28/CTLA-4:B7 pathway.<sup>4,5</sup> Similar to the condition of chronic viral infections, which maintain a relatively constant viral load, we have observed that coexpression of PD-1 and Tim-3 on CD8<sup>+</sup> T cells that accumulate in the tumor-associated environment in a model of advanced AML that continues to progress over time. The exhaustion phenotype was restricted to the CD8<sup>+</sup> T-cell population, likely because of the fact that the tumor cell line used in this study was MHC class I<sup>+</sup>, MHC class II<sup>-</sup>, gal-9<sup>+</sup>, and PDL1<sup>+</sup> with APC capacity, which favors a direct CD8<sup>+</sup> T-cell mediated immune response. Thus, the exhaustion phenotype may develop as the consequence of increasing

antigen load and tumor burden and provide a means by which AML cells subvert the immune system. Consistent with this hypothesis, Tim-3<sup>+</sup>PD-1<sup>+</sup> CD8<sup>+</sup> T cells had a predominant T-effector phenotype compared with Tim-3<sup>-</sup>PD-1<sup>-</sup> CD8<sup>+</sup> T cells in AML tumor-bearing mice suggesting that vigorous and perhaps chronic immune recognition of the tumor cells drives CD8<sup>+</sup> T cells into the exhaustion phenotype. In our AML model system, coblockade of PD-1 and Tim-3 reduced tumor burden and prolonged survival. Similarly, in mice with LCMV<sup>23</sup> or Friend leukemia infection<sup>24</sup> or those with solid tumors,<sup>25</sup> exhaustion also was associated with the coexpression of PD-1 and Tim-3 on CD8<sup>+</sup> T-effector cell types and in vivo coblockade of these 2 pathways augmented immune responses. Although the CD8<sup>+</sup> T-cell exhaustion phenotype was seen in tumor-infiltrating lymphocytes isolated from mice with colon adenocarcinoma, mammary adenocarcinoma, and melanoma, the proportionately higher frequency of the more profoundly exhausted PD-1<sup>+</sup>Tim-3<sup>+</sup> phenotype was not seen in the melanoma model.<sup>25</sup> In these solid tumor models, PD-1<sup>+</sup>Tim-3<sup>-</sup> cells were present in higher frequency than in our AML model (25%-50% vs 1%-3%, respectively). The PD-1<sup>+</sup>Tim-3<sup>-</sup> CD8<sup>+</sup> T cells were shown to be less exhausted and therefore might contain both effector T cells and exhausted T cells. No PD-1<sup>-</sup>Tim-3<sup>+</sup> CD8<sup>+</sup> T cells were seen in the solid tumor models and these cells were infrequent in the AML model (1%-3%) in WT but not PD-1 KO recipients in which a high frequency of these cells with an exhaustion profile could be observed. Thus, it is important to study different types of tumor model systems to determine which favor the exhaustion phenotype, as well as to interrogate patients with various solid tumors and hematologic malignancies to determine which may be most amenable to PD-1/PDL1 and Tim-3/gal-9 coblockade. The degree of CD8<sup>+</sup> T-cell dysfunction in these distinct tumor models involves not only poor IFN- $\gamma$  production as reported in the PD-1<sup>+</sup> CD8<sup>+</sup> T-cell subset in mice with chronic LCMV infection,<sup>5</sup> but also TNF- $\alpha$  and IL-2. A higher percentage of Tim-3-expressing CD8<sup>+</sup> T cells also was present in the liver of AML-bearing PD-1 KO versus WT mice, despite the relative resistance of PD-1 KO mice to challenge with AML cells. These data suggest that there may be a compensatory increase in Tim-3 expression in the absence of PD-1 that may contribute in part to the residual susceptibility of these mice to AML lethality and further indicate that PD-1 expression is not required for Tim-3 coexpression on exhausted CD8<sup>+</sup> T cells. Whereas both PD-1<sup>+</sup>Tim-3<sup>+</sup> T cells in WT mice and Tim-3<sup>+</sup> T cells in PD-1 KO mice were dysfunctional, they were different in their capacities for cytokine production. PD-1<sup>-</sup> and Tim-3-coexpressing T cells were deficient in all 3 cytokine (IFN- $\gamma$ , TNF- $\alpha$ , and IL-2) production, whereas Tim-3<sup>+</sup>PD-1<sup>-</sup> CD8<sup>+</sup> T cells maintained their IL-2 production. These data suggest that the PD-1/PDL1 signaling pathway plays a critical role in controlling T-cell proliferation through negative regulation of IL-2 secretion in Tim-3<sup>+</sup> CD8<sup>+</sup> T cells.

In addition to the immune regulatory effects of the interaction between Tim-3 on CD8<sup>+</sup> T cells and the gal-9 expressed on the AML line itself, 3 distinct subsets of cells in the host of AML-bearing mice expressed high levels of gal-9: myeloid cells, DCs, and myeloid-derived suppressor cells that were found in the liver, spleen, and BM of AML-bearing mice. AML induced accumulation of these gal-9-expressing cells with the exception of CD11b<sup>+</sup>Gr-1<sup>-</sup> cells in the spleen. Gal-9 can also be expressed by cell types other than APCs, such as lymphocytes.<sup>47,48</sup> The wide distribution of gal-9 may contribute to multiple immunomodulatory roles of gal-9 and Tim-3 signaling pathway. For example, studies have shown interaction between the gal-9 on lymphocytes

and the Tim-3 on APCs may have a positive role in DC maturation process,<sup>13,22</sup> while ligation of the gal-9 on APCs and the Tim-3 on lymphocytes have an opposite role as to tune down the immune response.<sup>15,35,36,46,49</sup> The function of the various gal-9<sup>+</sup> immunoregulatory cells seen in mice with advanced AML on the generation and function of CD8<sup>+</sup> T cells in this model is of interest and will require extensive future investigations beyond the scope of this study to clearly define the role of each.

The additive effects of combined in vivo blockade of the PD-1/PDL1 and Tim-3/gal-9 in reducing AML disease burden and prolonging survival was demonstrated in studies in which Tim3-Fc fusion protein and anti-PDL1 mAb were given to WT mice or anti-PDL1 mAb was given to gal-9 KO mice. The latter resulted in a more pronounced long-term survival than the former, which may be because of the incomplete blockade at sites of AML disease likely achieved with a fusion protein compared with the obligatory blockade of a KO mouse. However, because the AML tumor cells provide a source of gal-9 in the gal-9 KO mouse, in theory the fusion protein, if present at saturating concentrations in all the necessary locations, would be able to block all gal-9 availability although in practice achieving saturation at the tissue level with some fusion proteins can be very challenging.

Tim-3/gal-9 pathway appears to contribute to a lesser extent compared with the PD-1/PDL1 pathway in rendering CD8<sup>+</sup> T cells exhausted. Consistent with this hypothesis, mTim-3 hFc fusion protein given to WT mice had only a marginal effect on survival. Moreover, although an enhanced antitumor response was observed in gal-9 KO mice, the magnitude of the resistance in gal-9 KO was modest compared with PD-1 KO mice. Interestingly, despite the relatively higher level of Tim-3 expression in PD-1 KO mice and the up-regulation of Tim-3 and PD-1 in gal-9 KO mice, PD-1 KO mice appear to be more resistant than gal-9 KO mice to AML cells. Because Treg suppression is poorer in PD-1 KO vs WT but not gal-9 KO mice, we speculate that the superior outcome of PD-1 KO vs gal-9 KO mice may be because of a reduced level of Treg suppression in vivo seen in the former, which we have previously shown to be critical in inhibiting IFN- $\gamma$  production by anti-AML-reactive CD8<sup>+</sup> T cells in WT mice.<sup>26</sup> Regardless of the explanations, the impaired function of Tim-3<sup>+</sup> CD8<sup>+</sup> T cells in PD-1 KO mice and the prolonged survival in gal-9 KO mice with AML indicate that Tim-3/gal-9 pathway indeed contributes to the antitumor CD8<sup>+</sup> T-cell exhaustion phenotype.

The intense interest in studying T-cell exhaustion and its role in regulating antitumor response have led to recent studies in patients with metastatic melanoma. Those studies now have shown the presence of tumor-reactive PD-1<sup>+</sup>Tim-3<sup>+</sup> CD8<sup>+</sup> T cells indicative of an exhaustion phenotype. Specifically, peripheral blood tumor-reactive CD8<sup>+</sup> T cells isolated from stage IV melanoma patients coexpressed PD-1 and Tim-3 and, similar to rodent studies, had a more profound cytokine defect than their PD-1<sup>+</sup>Tim-3<sup>-</sup> T cells counterparts.<sup>41</sup> In vitro blockade of the Tim-3/gal-9 pathway was synergistic with PD-1/PDL1 pathway blockade in reversing CD8<sup>+</sup> T-cell exhaustion.<sup>41</sup> Taken together, these data indicate that mouse or human CD8<sup>+</sup> T cells exposed to high levels of tumor antigens can acquire a severely exhausted phenotype, regardless of whether the tumor begins as a solid tumor mass or as a hematologic malignancy. Most importantly, collectively these data provide the foundation of a novel therapy to restore the function of defeated antitumor T cells that may be useful in reducing AML tumor burden in the clinic should the PD-1<sup>+</sup>Tim-3<sup>+</sup> CD8<sup>+</sup> T-cell exhaustion profile be observed in AML patients at the site of disease.



## Acknowledgments

The authors thank Dr Terry Strom for providing the mTim-3 hFc protein.

This work was supported in part by National Institutes of Health grants R01 CA72669, R01AI34495, and P01056299, and the Children's Cancer Research Fund.

## Authorship

Contribution: Q.Z. designed, organized, and supervised research, performed experiments, analyzed data, designed the figures, and

wrote the paper; M.E.M. performed experiments; R.G.V. performed experiments and edited the paper; B.J.W., D.H.M., and W.J.M. designed research and edited the paper; M.A. provided the PD-L1 mAb hybridoma; M.H. provided gal-9 KO mice; A.C.A. and V.K.K. provided mTim-3 hFc, designed research, and edited the paper; and B.R.B. designed, organized, and supervised research and edited the paper.

Conflict-of-interest disclosure: The authors declare no competing financial interests.

Correspondence: Bruce R. Blazar, MD, Department of Pediatrics, MMC 109, University of Minnesota, Minneapolis, MN 55455; e-mail address: blaza001@umn.edu.

## References

- Zajac AJ, Blattman JN, Murali-Krishna K, et al. Viral immune evasion due to persistence of activated T cells without effector function. *J Exp Med*. 1998;188(12):2205-2213.
- Urbani S, Amadei B, Tola D, et al. PD-1 expression in acute hepatitis C virus (HCV) infection is associated with HCV-specific CD8 exhaustion. *J Virol*. 2006;80(22):11398-11403.
- Freeman GJ, Wherry EJ, Ahmed R, Sharpe AH. Reinvigorating exhausted HIV-specific T cells via PD-1-PD-1 ligand blockade. *J Exp Med*. 2006;203(10):2223-2227.
- Nakamoto N, Cho H, Shaked A, et al. Synergistic reversal of intrahepatic HCV-specific CD8 T cell exhaustion by combined PD-1/CTLA-4 blockade. *PLoS Pathog*. 2009;5(2):e1000313.
- Barber DL, Wherry EJ, Masopust D, et al. Restoring function in exhausted CD8 T cells during chronic viral infection. *Nature*. 2006;439(7077):682-687.
- Golden-Mason L, Palmer B, Klarquist J, Mengshol JA, Castelblanco N, Rosen HR. Up-regulation of PD-1 expression on circulating and intrahepatic hepatitis C virus-specific CD8<sup>+</sup>T cells associated with reversible immune dysfunction. *J Virol*. 2007;81(17):9249-9258.
- Day CL, Kaufmann DE, Kiepiela P, et al. PD-1 expression on HIV-specific T cells is associated with T-cell exhaustion and disease progression. *Nature*. 2006;443(7109):350-354.
- Ahmadzadeh M, Johnson LA, Heemskerk B, et al. Tumor antigen-specific CD8 T cells infiltrating the tumor express high levels of PD-1 and are functionally impaired. *Blood*. 2009;114(8):1537-1544.
- Gehring AJ, Ho ZZ, Tan AT, et al. Profile of tumor antigen-specific CD8 T cells in patients with hepatitis B virus-related hepatocellular carcinoma. *Gastroenterology*. 2009;137(2):682-690.
- Yamamoto R, Nishikori M, Kitawaki T, et al. PD-1/PD-1 ligand interaction contributes to immunosuppressive microenvironment of Hodgkin lymphoma. *Blood*. 2008;111(6):3220-3224.
- Zhang L, Gajewski TF, Kline J. PD-1/PD-L1 interactions inhibit antitumor immune responses in a murine acute myeloid leukemia model. *Blood*. 2009;114(8):1545-1552.
- Wang F, He W, Zhou H, et al. The Tim-3 ligand galectin-9 negatively regulates CD8<sup>+</sup> alloreactive T cell and prolongs survival of skin graft. *Cell Immunol*. 2007;250(1-2):68-74.
- Anderson AC, Anderson DE, Bregoli L, et al. Promotion of tissue inflammation by the immune receptor Tim-3 expressed on innate immune cells. *Science*. 2007;318(5853):1141-1143.
- Jones RB, Ndhlovu LC, Barbour JD, et al. Tim-3 expression defines a novel population of dysfunctional T cells with highly elevated frequencies in progressive HIV-1 infection. *J Exp Med*. 2008;205(12):2763-2779.
- Zhu C, Anderson AC, Schubart A, et al. The Tim-3 ligand galectin-9 negatively regulates T helper type 1 immunity. *Nat Immunol*. 2005;6(12):1245-1252.
- Cao E, Zang X, Ramagopal UA, et al. T cell immunoglobulin mucin-3 crystal structure reveals a galectin-9-independent ligand-binding surface. *Immunity*. 2007;26(3):311-321.
- Wilker PR, Sedy JR, Grigura V, Murphy TL, Murphy KM. Evidence for carbohydrate recognition and homotypic and heterotypic binding by the TIM family. *Int Immunol*. 2007;19(6):763-773.
- Rabinovich GA, Rubinstein N, Toscano MA. Role of galectins in inflammatory and immunomodulatory processes. *Biochim Biophys Acta*. 2002;1572(2-3):274-284.
- Seki M, Oomizu S, Sakata KM, et al. Galectin-9 suppresses the generation of Th17, promotes the induction of regulatory T cells, and regulates experimental autoimmune arthritis. *Clin Immunol*. 2008;127(1):78-88.
- Sabatos CA, Chakravarti S, Cha E, et al. Interaction of Tim-3 and Tim-3 ligand regulates T helper type 1 responses and induction of peripheral tolerance. *Nat Immunol*. 2003;4(11):1102-1110.
- Sanchez-Fueyo A, Tian J, Picarella D, et al. Tim-3 inhibits T helper type 1-mediated auto- and alloimmune responses and promotes immunological tolerance. *Nat Immunol*. 2003;4(11):1093-1101.
- Nagahara K, Arikawa T, Oomizu S, et al. Galectin-9 increases Tim-3<sup>+</sup> dendritic cells and CD8<sup>+</sup>T cells and enhances antitumor immunity via galectin-9-Tim-3 interactions. *J Immunol*. 2008;181(11):7660-7669.
- Jin HT, Anderson AC, Tan WG, et al. Cooperation of Tim-3 and PD-1 in CD8 T-cell exhaustion during chronic viral infection. *Proc Natl Acad Sci U S A*. 2010;107(33):14733-14738.
- Takamura S, Tsuji-Kawahara S, Yagita H, et al. Premature terminal exhaustion of Friend virus-specific effector CD8<sup>+</sup>T cells by rapid induction of multiple inhibitory receptors. *J Immunol*. 2010;184(9):4696-4707.
- Sakuishi K, Apetoh L, Sullivan JM, Blazar BR, Kuchroo VK, Anderson AC. Targeting Tim-3 and PD-1 pathways to reverse T cell exhaustion and restore antitumor immunity. *J Exp Med*. 2010;207(10):2187-94.
- Zhou Q, Munger ME, Highfill SL, et al. Program death-1 signaling and regulatory T cells collaborate to resist the function of adoptively transferred cytotoxic T lymphocytes in advanced acute myeloid leukemia. *Blood*. 2010;116(14):2484-2493.
- Seki M, Sakata KM, Oomizu S, et al. Beneficial effect of galectin 9 on rheumatoid arthritis by induction of apoptosis of synovial fibroblasts. *Arthritis Rheum*. 2007;56(12):3968-3976.
- Tsuboi Y, Abe H, Nakagawa R, et al. Galectin-9 protects mice from the Shwartzman reaction by attracting prostaglandin E2-producing polymorphonuclear leukocytes. *Clin Immunol*. 2007;124(2):221-233.
- Nishimura H, Minato N, Nakano T, Honjo T. Immunological studies on PD-1 deficient mice: implication of PD-1 as a negative regulator for B cell responses. *Int Immunol*. 1998;10(10):1563-1572.
- Sauer MG, Ericson ME, Weigel BJ, et al. A novel system for simultaneous in vivo tracking and biological assessment of leukemia cells and ex vivo generated leukemia-reactive cytotoxic T cells. *Cancer Res*. 2004;64(11):3914-3921.
- Zhou Q, Bucher C, Munger ME, et al. Depletion of endogenous tumor-associated regulatory T cells improves the efficacy of adoptive cytotoxic T-cell immunotherapy in murine acute myeloid leukemia. *Blood*. 2009;114(18):3793-3802.
- Rosignoli G, Lim CH, Bower M, Gotch F, Imami N. Programmed death (PD)-1 molecule and its ligand PD-L1 distribution among memory CD4 and CD8 T cell subsets in human immunodeficiency virus-1-infected individuals. *Clin Exp Immunol*. 2009;157(1):90-97.
- Wherry EJ, Ha SJ, Kaech SM, et al. Molecular signature of CD8<sup>+</sup>T cell exhaustion during chronic viral infection. *Immunity*. 2007;27(4):670-684.
- Mumprecht S, Schurch C, Schwaller J, Solenthaler M, Ochsenbein AF. Programmed death 1 signaling on chronic myeloid leukemia-specific T cells results in T-cell exhaustion and disease progression. *Blood*. 2009;114(8):1528-1536.
- Wang F, He W, Yuan J, et al. Activation of Tim-3-Galectin-9 pathway improves survival of fully allogeneic skin grafts. *Transpl Immunol*. 2008;19(1):12-19.
- Arikawa T, Watanabe K, Seki M, et al. Galectin-9 ameliorates immune complex-induced arthritis by regulating Fc gamma R expression on macrophages. *Clin Immunol*. 2009;133(3):382-392.
- Katoh S, Ishii N, Nobumoto A, et al. Galectin-9 inhibits CD44-hyaluronan interaction and suppresses a murine model of allergic asthma. *Am J Respir Crit Care Med*. 2007;176(1):27-35.
- Wiener Z, Kohalmi B, Pocza P, et al. TIM-3 is expressed in melanoma cells and is upregulated in TGF-beta stimulated mast cells. *J Invest Dermatol*. 2007;127(4):906-914.
- Dardalhon V, Anderson AC, Karman J, et al. Tim-3/galectin-9 pathway: regulation of Th1 immunity through promotion of CD11b<sup>+</sup>Ly-6G<sup>+</sup> myeloid cells. *J Immunol*. 2010;185(3):1383-1392.
- Wada J, Kanwar YS. Identification and characterization of galectin-9, a novel beta-galactoside-binding mammalian lectin. *J Biol Chem*. 1997;272(9):6078-6086.
- Fourcade J, Sun Z, Benallaoua M, et al. Upregulation of Tim-3 and PD-1 expression is associated with tumor antigen-specific CD8<sup>+</sup>T cell dysfunction in melanoma patients. *J Exp Med*. 2010;207(10):2175-86.

42. Irie A, Yamauchi A, Kontani K, et al. Galectin-9 as a prognostic factor with antimetastatic potential in breast cancer. *Clin Cancer Res*. 2005;11(8):2962-2968.
43. Nobumoto A, Nagahara K, Oomizu S, et al. Galectin-9 suppresses tumor metastasis by blocking adhesion to endothelium and extracellular matrices. *Glycobiology*. 2008;18(9):735-744.
44. Asakura H, Kashio Y, Nakamura K, et al. Selective eosinophil adhesion to fibroblast via IFN-gamma-induced galectin-9. *J Immunol*. 2002;169(10):5912-5918.
45. Imaizumi T, Kumagai M, Sasaki N, et al. Interferon-gamma stimulates the expression of galectin-9 in cultured human endothelial cells. *J Leukoc Biol*. 2002;72(3):486-491.
46. Wang F, Wan L, Zhang C, Zheng X, Li J, Chen ZK. Tim-3-Galectin-9 pathway involves the suppression induced by CD4<sup>+</sup>CD25<sup>+</sup> regulatory T cells. *Immunobiology*. 2009;214(5):342-349.
47. Kuchroo VK, Dardalhon V, Xiao S, Anderson AC. New roles for TIM family members in immune regulation. *Nat Rev Immunol*. 2008;8(8):577-580.
48. Rodriguez-Manzanet R, DeKruyff R, Kuchroo VK, Umetsu DT. The costimulatory role of TIM molecules. *Immunol Rev*. 2009;229(1):259-270.
49. Liang M, Ueno M, Oomizu S, et al. Galectin-9 expression links to malignant potential of cervical squamous cell carcinoma. *J Cancer Res Clin Oncol*. 2008;134(8):899-907.